Available online at www.sciencedirect.com

Journal of Crystal Growth 249 (2003) 179–185

JOURNAL OF CRYSTAL GROWTH

www.elsevier.com/locate/jcrysgro

Effects of RF power on properties of ZnO thin films grown on Si (0 0 1) substrate by plasma enhanced chemical vapor deposition

B.S. Li[a], Y.C. Liu[a,b,*], D.Z. Shen[a], J.Y. Zhang[a], Y.M. Lu[a], X.W. Fan[a]

[a] *Key Laboratory of Excited State Processes, Changchun Institute of Optics, Fine Mechanics and Physics, Chinese Academy of Sciences, 1-Yan An Road Changchun 130021, China*

[b] *Center for Opto-electronic Functional Material Research, Northeast University, Changchun 130024, China*

Received 3 April 2002; accepted 12 October 2002
Communicated by R. James

Abstract

ZnO thin films have been grown on Si(1 0 0) substrate by plasma enhanced chemical vapor deposition (PECVD) using a zinc organic source (DEZ) and carbon dioxide (CO_2) gas mixture at a low temperature. It is demonstrated that the radio frequency (RF) plasma power can dramatically effect the properties of ZnO thin films. The quality of ZnO thin films was studied by X-ray diffraction (XRD), atomic force microscopy (AFM), and photoluminescence spectra (PL). Under the optimized condition of RF power of 19 W, a *c*-axis-orientated wurtize structure ZnO thin film with the XRD full-width at half-maximum (FWHM) of 0.21° was prepared, and a strong free excitonic emission with a narrow PL FWHM of 90 meV at 3.286 eV was observed. The origin of the UV band is the free exciton recombination, as verified by temperature dependent PL spectra.

PACS: 81.15.Gh; 78.66.Hf; 78.70.Ck; 78.55.Et

Keywords: A1. Photoluminescence; A3. Plasma enhanced chemical vapor deposition; A3. ZnO thin films; B1. Diethylzinc

1. Introduction

Zinc oxide (ZnO), a wide band gap semiconductor ($E_g = 3.4$ eV) with a large excitonic binding energy of 60 meV has been recognized as a promising material for use in ultraviolet light emission devices and laser diodes. Recently, the optically pumped stimulated emission of ZnO thin films has been reported [1–5], making it a hotspot in the optoelectronic material and devices, as a promising candidate for realizing the short-wavelength light-emitting devices (LEDs). Furthermore, ZnO devices should not suffer from dislocation degradation during operation, as it is

---

*Corresponding author. Key Laboratory of Excited State Processes, Changchun Institute of Optics, Fine Mechanics and Physics, Chinese Academy of Sciences, 1-Yan An Road Changchun 130021, China. Tel.: +86-0431-5937596; fax: +86-0431-5955378.

E-mail address: ycliu@nenu.edu.cn (Y.C. Liu).

0022-0248/03/$ - see front matter © 2002 Elsevier Science B.V. All rights reserved.
PII: S0022-0248(02)02069-9

one of the "hardest" materials in the II–VI compound family [6].

In the present paper, we employ a plasma enhanced chemical vapor deposition technology (PECVD) to prepare ZnO thin films on a Si(1 0 0) substrate. An obvious advantage of the method is to grow thin films at low temperature. This is because the chemical reactants can be easily activated by the radio frequency electron-magnetic field. Generally, the thin-film quality is closely dependent on the temperature of the substrate (TS), the gas flow rate ratio of $Zn(C_2H_5)_2$ (DEZ) to CO_2 (GFRRZC), and in particular, the radio frequency (RF) power. The relationships of the properties of ZnO thin films with TS and GFRRZC have been studied in detail [7,8]. However, the effects of RF power on the characteristics of ZnO thin films have not been sufficiently investigated. A series of samples with different RF powers were prepared to investigate the effect of the radio frequency (RF) power on the properties of ZnO thin films. The properties of the ZnO thin films were studied employing X-ray diffraction (XRD), atomic force microscopy (AFM) and photoluminescence spectra (PL). The origin of the UV band is from the free exciton recombination, which was determined by the temperature dependent PL spectra.

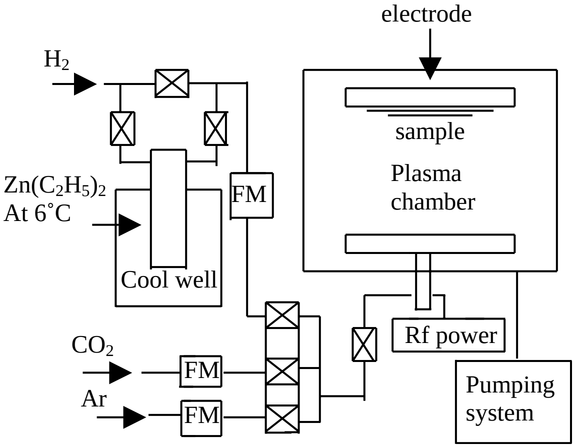

Fig. 1. Schematic diagram of the plasma enhanced chemical vapor deposition.

2. Experimental procedure

ZnO thin films are grown by PECVD from the gas mixture of diethylzinc and carbon dioxide. The schematic structure of the PECVD system is shown in Fig. 1, which has the 15-cm diameter parallel-faced electrodes for the capacitive coupling discharge. The chamber size is 22 cm in diameter and 21 cm in height. The electrode spacing is 3 cm, and the discharge is observed to be almost uniform throughout the 15-cm diameter electrode area. The gas flow rates are controlled by different gas flowmeters. The DEZ source is packed in a steel cylinder cooled to 20°C by a CW-1 type fine controlled temperature semiconductor device. High-purity hydrogen is used as the carrier gas for carrying DEZ into the reactive chamber. CO_2 does not react with DEZ at room temperature. Thus, CO_2 can be blended adequately with DEZ before they enter the plasma chamber. The Si substrates are chemically treated by a standard RCA process [9]. The background pressure is less than 4×10^{-4} Pa in the reactor chamber. Argon and hydrogen are filled into the plasma chamber sequentially. After the Si substrate is heated, which is measured by a copper–constantan thermocouple, RF power is loaded into the chamber. The argon and hydrogen plasmas generated by the RF in the plasma chamber are used to clean the Si surface. The cleaning of Si surface was carried out by a three-step process. At first, the argon and hydrogen plasmas induced from the RF with a power of 80 W in the chamber are used to remove the oxide layer. A 30 min processing time is used for oxide cleaning. Secondly, ammonia gas is introduced into the plasma chamber to nitridate the Si surface for 15 min [8]. Then the RF power is adjusted to a determined value to grow the ZnO thin films.

In order to investigate the effects of RF power on the quality of ZnO thin films, a series of samples were grown on Si substrates with different RF powers. The detailed growth conditions are listed in Table 1.

The crystalline quality of the ZnO layers was examined by XRD using a rotating anode X-ray diffractometer with Cu $K_{\alpha 1}$ radiation of 1.54 Å. The topography of the thin film was imaged under

Table 1
The deposition conditions of ZnO thin films with changing the RF power.

Sample	(RF) power (W)	Temperature of the substrate (°C)	Gas flow ratio of $Zn(C_2H_5)_2$ to CO_2
A	6	230	1:1
B	14	230	1:1
C	19	230	1:1
D	35	230	1:1
E	50	230	1:1
F	70	230	1:1

ambient air with a convention AFM (Park Scientific Instrument Co.).The PL spectra were measured using a UV Labran Infinity Spectrophotometer (J-Y Company, French) excited by a continuous He–Cd laser with an output power of 30 mW. The PL signals were detected by a CCD camera with a high resolution of 0.04 nm. Measurements were taken in the range of 83–580 K by placing the sample cells in a cryogenic unit.

3. Results and discussion

Fig. 2(a–f) show the X-ray diffraction patterns of the ZnO thin films prepared by PECVD with different RF powers. At a RF power of 6 W, there is a dominating (0 0 2) peak and a very weak (1 0 1) peak, as shown in Fig. 2(a). With increasing RF power, the intensity of the (1 0 1) peak significantly decreases, as shown in Fig. 2(b). When the RF power reaches 19 W, the peak of (1 0 1) disappeared and only a (0 0 2) peak of ZnO appeared, as shown in Fig. 2(c). If we further increased the RF power to 35, 50 and 70 W, the diffraction intensity of (0 0 2) decreased and the (1 0 0), (1 0 1), (1 0 2), (1 1 2), and (1 0 3) diffraction peaks reappeared, as shown in Fig. 2(d–f). Additionally, the full-width at half-maximum (FWHM) of the (0 0 2) ZnO peak at 34.42° is closely dependent on the RF power. FWHMs of samples A–F are 0.37°, 0.24°, 0.21°, 0.35°, 0.37°, and 0.34°, respectively. The mean grain size, d, is calculated by employing the Scherrer formula [10]. According to this formula, the mean grain sizes of samples A–F are 23.5, 36.2, 41.4, 24.9, 23.5 and 25.5 nm, respectively. The PECVD technology employs a glow discharge to generate active species such as ions, atoms, molecules or free radicals. At low RF power, ZnO thin films look faint yellow. This is because the low RF power cannot produce enough active oxygen, resulting form the large bond energy of CO_2. When the RF power increases to 19 W, the active oxygen increases, the films become clean-cut, and the color of yellow disappears. It is known that the surface free energy of semiconductors strongly depends on the hybridized orbit [11]. When the ZnO film was deposited onto a substrate without the influence of epitaxy, the surface of a film tends to be (0 0 2) plane, because this plane has a minimum surface free energy. Of course, this model is appropriate for the case where the atomic diffusion is large at the out surface of the growing film [12]. Increasing the input RF power can enhance the mobility of species on the substrate [13]. This can be understood by the following processes. The running ions can collide with the

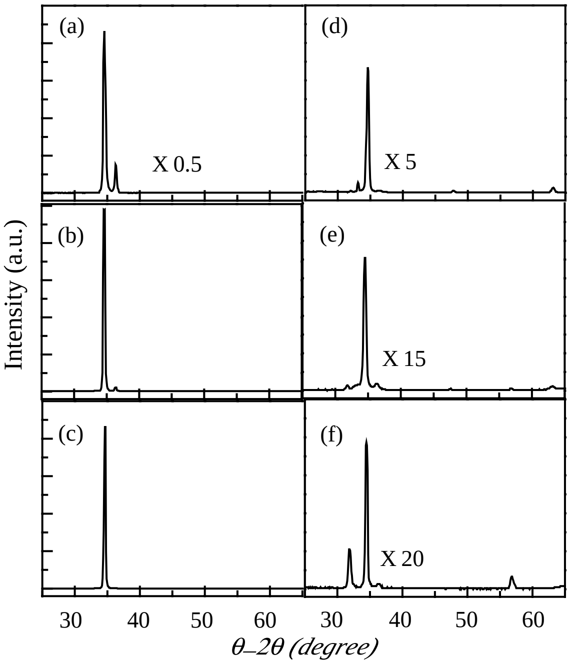

Fig. 2. X-ray diffraction patterns of the ZnO thin films grown on Si(1 0 0) substrates with changing RF power: (a) 6 W; (b) 14 W; (c) 19 W; (d)35 W; (e) 50 W; (f) 70 W.

adsorbed species and exchange the momentum with each other; the UV irradiation can enhance the mobility of adsorbed species [14]. Thus, an increasing of RF power results in the decrease of the (1 0 1) peak and the formation of a full c-axis orientated ZnO thin film. However, if the input RF power further increases, the crystal quality of the ZnO thin films becomes poor. This may be due to a faster reactive rate and surface damage by the bombardment of more energetic particles.

The dependence of the morphology of ZnO thin films on the input RF power was investigated using atomic force microscopy. In this experiment, we find that the surface roughness and the grain shape of ZnO thin films are closely related to the RF power, as shown in Fig. 3(a–f). At low RF power, columnar ZnO grains stand perpendicular to the substrate, as shown in Fig. 3(a) and (b). For an input RF power of 19 W, the film exhibits a smooth surface. However, the surface becomes rough with further increasing of RF power, and the grain shape becomes irregular. From Fig. 3, it can be deduced that film densification and surface damage induced by plasma bombardment and ultraviolet ray irradiation are related to the RF power.

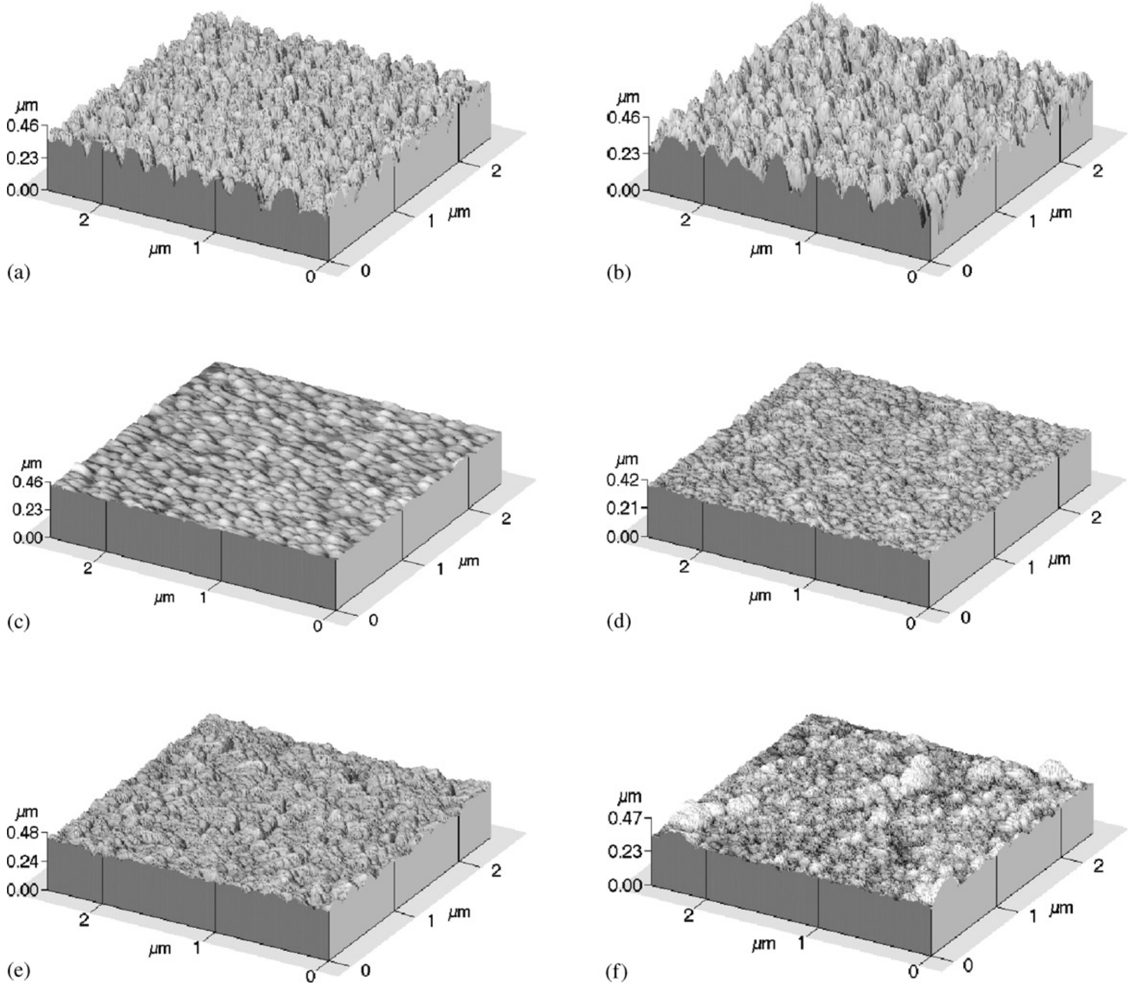

Fig. 3. AFM images of ZnO thin films prepared at different of RF powers: (a) 6 W; (b) 14 W; (c) 19 W; (d) 35 W; (e) 50 W; (f) 70 W.

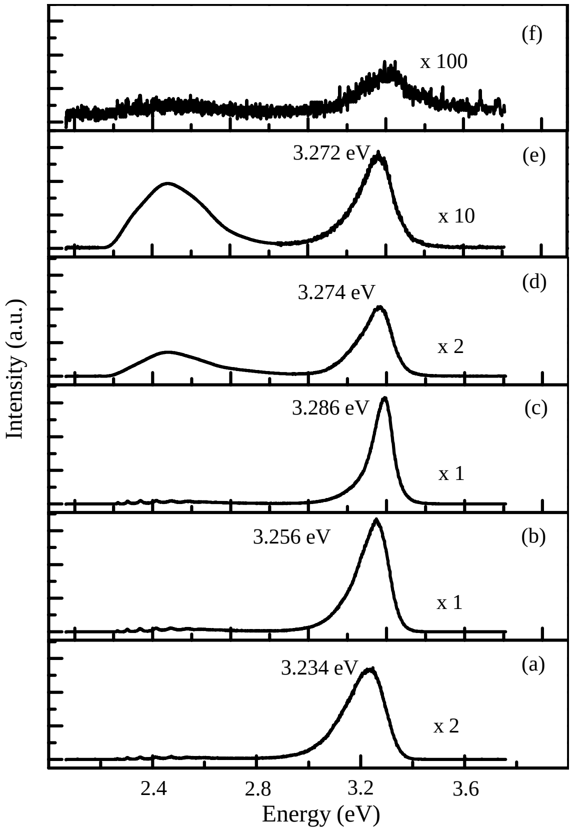

Fig. 4. PL spectra of ZnO thin films prepared at different RF power: (a) 6 W; (b) 14 W; (c) 19 W; (d) 35 W; (e) 50 W; (f) 70 W.

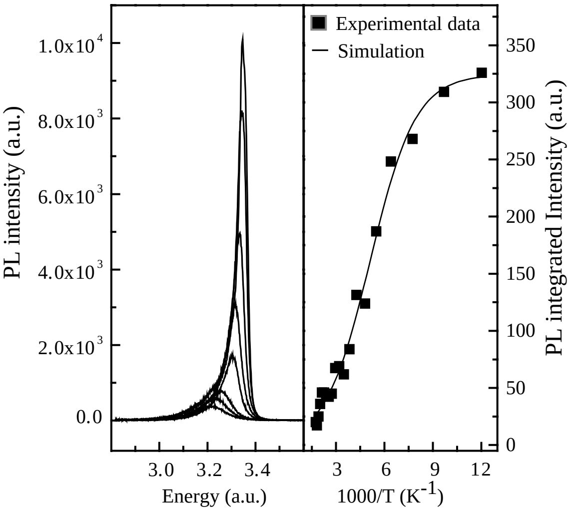

Fig. 5. Left: The PL spectra of sample C (prepared at an input RF power of 19 W) at different temperatures (a). Right: the integrated PL intensity dependence on the temperature (b). The square data points are experimental points simulated by the theoretical formula, equation $I(T) = I_0/1 + A\exp(-\Delta E/k_B T)$.

Fig. 4(a–f) show the PL spectra of the ZnO thin films measured at room temperature. For the PL spectra, the main emission properties were closely dependent on the RF power. With the low RF power, only an UV band can be seen in the PL spectra, as shown in Fig. 5(a–c). With increasing RF power, a visible band appears and becomes strong while the UV band decreases. When the input RF power is 70 W, the UV band as well as the visible band is drastically quenched, as shown in Fig. 4(f). Generally, it is accepted that the origin of visible band is relative to oxygen vacancies [15]. Increasing RF power results in creating more oxygen vacancies. In III–V semiconductors, energetic ion bombardment can induce preferential sputtering of the relatively light atom, resulting in a nonstoichiometric surface [16,17]. In our experiment, the growth of ZnO thin film is carried out in plasma, which is accompanied by energetic ion bombardment. With the increase of RF power, enhanced high energetic ion bombardment leads to damage, and the quality of ZnO thin film will become poorer. Thus, the oxygen atom will be preferentially lost in the film, and defects will be generated by the sputtering of running ions [18]. The FWHMs of the PL spectra of samples A to F are 159, 129, 90, 137, and 158 meV, respectively. The linewidth measured at room temperature is 90 meV which is much narrower than the results of 120, 117, 109 meV that have been previously reported [8,19,20]. The peak positions of the UV band change between 3.234 and 3.286 eV, as shown in Fig. 4. The UV band of sample A is from a bound exciton, while the origin is a free exciton in sample C. This conclusion was reached by the temperature dependent PL spectra, as discussed in the next section. Here, we think the UV band was overlapped by free exciton and bound exciton recombination for samples B, D, and E, because their characteristics stand between samples A and C. With improving quality of the ZnO thin film, the density of defects was reduced,

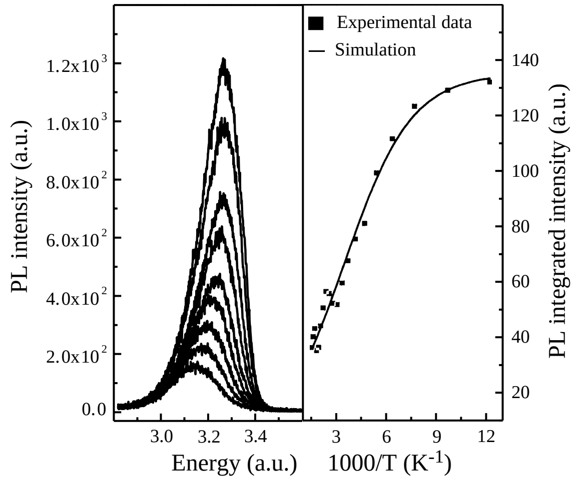

Fig. 6. Left: The PL spectra of sample A (prepared at an input RF power of 6 W) at different temperatures (a). Right: the integrated PL intensity dependence on the temperature (b). The square data points are experimental points simulated by the theoretical formula.

resulting in a narrower FWHM as well as a blue shift in the UV band.

To provide more information to understand the origin of the UV emission, we studied the optical properties of samples A and C at various temperatures. Fig. 5(a) shows the temperature dependent PL spectra of sample C in the range of 80 to 580 K. In Fig. 5(a), the peak intensity of the UV band increases significantly with decreasing temperature. The intensity at 83 K is 26 times higher than that at 573 K. Fig. 5(b) is the temperature dependence of the integrated PL intensity of sample C. Generally, the thermal quenching of luminescence intensity can be expressed as [21,22]

$$I(T) = \frac{I_0}{1 + A\exp(-\Delta E/k_B T)}, \tag{1}$$

where ΔE is the activation energy of the thermal quenching process, k_B is Boltaman constant, I_0 is the emission intensity at 0 K, T is the thermodynamic temperature, and A is a constant. When using this theoretical formula to fit our experimental data, as shown Fig. 5(b), we get ΔE as 61.9 meV. This value is in agreement with the exciton binding energy of 60 meV in bulk ZnO crystal. Thus, we can conclude that the UV band of sample C is from free exciton recombination. In contrast to sample C, the intensity of the UV band in sample A does not show as large of a temperature dependence, i.e. the peak intensity of the UV band is only 5 times higher at 83 K than that at 573 K, as shown in Fig. 6(a). The activation energy, ΔE, is 44.3 meV by simulating the experimental data with Eq. (1), which is obviously different from the free excitonic binding energy of 60 meV in bulk ZnO. So we conclude the UV band in sample A is from bound exciton recombination.

4. Conclusion

ZnO thin films have been grown on Si(0 0 1) substrates at low temperature. It has been shown that the RF power affects the quality of the ZnO thin films. The crystal quality, as well as the morphology of the surface and the optical properties of ZnO thin films, are dependent on the RF power. The plasma can induce a process of film densification, and it can also damage the film at high RF power. At the optimal RF power of 19 W, a *c*-axis orientated ZnO thin film with a smooth surface and an excellent free exciton emission was obtained.

Acknowledgements

This work was supported by the Program of CAS Hundred Talents, the National Fundamental and Applied Research Project, the National Natural Science Foundation of China, the innovation foundation of CIOFP, Excellent Young Teacher Foundation of Ministry of Education of China, and Jilin Distinguished Young Scholar Program.

References

[1] D.C. Reynolds, D.C. Look, B. Jogai, Solid State Commun. 99 (1996) 873.
[2] D.M. Bagnall, Y.F. Chen, Z. Zhu, T. Yao, S. Koyama, M.Y. Shen, T. Goto, Appl. Phys. Lett. 70 (1997) 2230.

[3] T.K. Tang, G.K.L. Wong, P. Yu, M. Kawasaki, A. Ohtomo, H. Koinuma, Y. Segawa, Appl. Phys. Lett. 72 (1998) 3270.

[4] M.H. Huang, S. Mao, H. Feick, H. Yan, Y. Wu, H. Kind, E. Weber, R. Russo, P. Yang, Science 292 (2001) 1897.

[5] X.T. Zhang, Y.C. Liu, L.G. Zhang, J.Y. Zhang, Y.M. Lu, D.Z. Shen, W. Xu, G.Z. Zhong, X.W. Fan, X.G. Kong, Chin. Phys. Lett. 19 (2002) 127.

[6] Y.F. Chen, D.M. Bagnall, H.J. Koh, K.T. Park, K. Hiraga, Z.Q. Zhu, T. Yao, J. Appl. Phys. 84 (1998) 3912.

[7] B.S. Li, Y.C. Liu, D.Z. Shen, Y.M. Lu, J.Y. Zhang, X.G. Kong, X.W. Fan, Z.Z. Zhi, J. Vac. Sci. Technol. A 20 (2002) 265.

[8] B.S. Li, Y.C. Liu, Z.S. Chu, D.Z. Shen, Y.M. Lu, J.Y. Zhang, X.W. Fan, J. Appl. Phys. 91 (2002) 501.

[9] W. Kern, D.A. Puotinen, RCA Rev. 31 (1970) 187.

[10] W.T. Lim, C.H. Lee, Thin Solid Films 353 (1999) 12.

[11] N. Fujinura, T. Nishihara, S. Goto, J.F. Xu, T. Ito, J. Crystal Growth 130 (1993) 269.

[12] G. Knuyt, C. Quaeyhaegens, J. D'Haen, L.M. Stals, Thin Solid Films 258 (1995) 159.

[13] Y.G. Kim, H.J. Kim, Mater. Lett. 21 (1994) 351.

[14] M. Shimizu, H. Kamei, M. Tanizawa, T. Shiosaki, A. Kawabata, J. Crystal Growth 89 (1988) 365.

[15] K. Vanheusden, W.L. Warren, C.H. Seager, D.R. Tallant, J.A. Voigt, B.E. Gnade, J. Appl. Phys. 79 (1996) 7983.

[16] J.M. Lee, K.M. Chang, S.W. Kim, C. Huh, I.H. Lee, S.J. Park, Appl. Phys. Lett. 87 (2000) 7667.

[17] S.J. Pearton, U.K Chakrabarti, F.A. Baiocchi, Appl. Phys. Lett. 55 (1989) 1633.

[18] J.M. Lee, K.K. Kim, S.J. Park, W.K. Choi, Appl. Phys. Lett. 78 (2001) 3842.

[19] A.B.M. Almamun Ashrafi, A. Ueta, A. Avramescu, H. Kumano, Y.W. Ok, T.Y. Seong, Appl. Phys. Lett. 76 (2000) 550.

[20] M.A.L. Johnson, S. Fugita, W.H. Rowland, W.C. Hughes, J.W. Cook, J.F. Schetzina, J. Electron. Mater. 25 (1996) 855.

[21] P.O. Holtz, B. Monemar, H.J. Lozykowski, Phys. Rev. B. 32 (1985) 986.

[22] D.S. Jiang, H. Jung, K. Ploog, J. Appl. Phys. 64 (1988) 1371.